

ARMY RESEARCH LABORATORY



Simulation of Adaptive Seat Energy Absorber for Military Rotorcraft Crash Safety Enhancement

by Muthuvel Murugan, JinHyeong Yoo, and Gregory Hiemenz

ARL-TR-6892

April 2014

NOTICES

Disclaimers

The findings in this report are not to be construed as an official Department of the Army position unless so designated by other authorized documents.

Citation of manufacturer's or trade names does not constitute an official endorsement or approval of the use thereof.

Destroy this report when it is no longer needed. Do not return it to the originator.

Army Research Laboratory

Aberdeen Proving Ground, MD 21005-5069

ARL-TR-6892

April 2014

Simulation of Adaptive Seat Energy Absorber for Military Rotorcraft Crash Safety Enhancement

Muthuvel Murugan and JinHyeong Yoo
Vehicle Technology Directorate, ARL

Gregory Hiemenz
InnoVital Systems Inc., Beltsville, MD

REPORT DOCUMENTATION PAGE			Form Approved OMB No. 0704-0188	
<p>Public reporting burden for this collection of information is estimated to average 1 hour per response, including the time for reviewing instructions, searching existing data sources, gathering and maintaining the data needed, and completing and reviewing the collection information. Send comments regarding this burden estimate or any other aspect of this collection of information, including suggestions for reducing the burden, to Department of Defense, Washington Headquarters Services, Directorate for Information Operations and Reports (0704-0188), 1215 Jefferson Davis Highway, Suite 1204, Arlington, VA 22202-4302. Respondents should be aware that notwithstanding any other provision of law, no person shall be subject to any penalty for failing to comply with a collection of information if it does not display a currently valid OMB control number.</p> <p>PLEASE DO NOT RETURN YOUR FORM TO THE ABOVE ADDRESS.</p>				
1. REPORT DATE (DD-MM-YYYY)	2. REPORT TYPE		3. DATES COVERED (From - To)	
April 2014	Final		1 October 2013–31 January 2014	
4. TITLE AND SUBTITLE			5a. CONTRACT NUMBER	
Simulation of Adaptive Seat Energy Absorber for Military Rotorcraft Crash Safety Enhancement			5b. GRANT NUMBER	
			5c. PROGRAM ELEMENT NUMBER	
6. AUTHOR(S)			5d. PROJECT NUMBER	
Muthuvvel Murugan, JinHyeong Yoo, and Gregory Hiemenz*			JASP# V-13-02	
			5e. TASK NUMBER	
			5f. WORK UNIT NUMBER	
7. PERFORMING ORGANIZATION NAME(S) AND ADDRESS(ES)			8. PERFORMING ORGANIZATION REPORT NUMBER	
U.S. Army Research Laboratory ATTN: RDRL-VTM Aberdeen Proving Ground, MD 21005-5069			ARL-TR-6892	
9. SPONSORING/MONITORING AGENCY NAME(S) AND ADDRESS(ES)			10. SPONSOR/MONITOR'S ACRONYM(S)	
			11. SPONSOR/MONITOR'S REPORT NUMBER(S)	
12. DISTRIBUTION/AVAILABILITY STATEMENT				
Approved for public release; distribution is unlimited.				
13. SUPPLEMENTARY NOTES				
* InnoVital Systems Inc., Beltsville, MD				
14. ABSTRACT				
This report documents the research study conducted on the analytical evaluation of magneto-rheological (MR) dampers for enhanced occupant protection during vertical crash landings of a helicopter. The current state-of-the-art helicopter crew seat has passive safety mechanisms that are highly limited in their capability to optimally adapt to each type of crash scenario due to variations in both occupant weight and crash severity level. While passive crash energy absorbers work well for a single design condition (50th percentile male occupant and fixed crash severity level), they do not offer adequate protection across a broad spectrum of crash conditions by minimizing the load transmitted to the occupant. This study reports the development of a lumped-parameter human body model including lower leg in a seated posture for rotorcraft crash injury simulation. The injury criteria and tolerance levels for the biomechanical effects are discussed for each of the identified vulnerable body regions, such as the thoracic lumbar loads for different sized adults. The desired objective of this analytical model development is to develop a tool to study the performance of adaptive semi-active magnetorheological seat suspensions for rotorcraft occupant protection.				
15. SUBJECT TERMS				
adaptive seat energy absorber, rotorcraft crash safety, active crash safety seat, multi-body seated human model				
16. SECURITY CLASSIFICATION OF:		17. LIMITATION OF ABSTRACT	18. NUMBER OF PAGES	19a. NAME OF RESPONSIBLE PERSON
a. REPORT	b. ABSTRACT	c. THIS PAGE	UU	Muthuvvel Murugan
Unclassified	Unclassified	Unclassified		
			28	19b. TELEPHONE NUMBER (Include area code)
				(410) 278-7903

Contents

List of Figures	iv
List of Tables	v
Acknowledgments	vi
1. Summary	1
2. Introduction	2
3. Model Development	3
4. Biodynamic Evaluation of Seated Human Model	5
4.1 STH Transmissibility (TR).....	6
4.2 DPM Impedance (IM)	6
5. Control Algorithm Development	7
6. Rotorcraft Crash Pulse	9
7. Injury Assessment Criteria	10
8. Simulation Results and Discussion	11
9. Concluding Remarks from Multi-Body Simulations	14
10. Finite-Element Model Development	14
11. Future Work	16
12. References	17
List of Symbols, Abbreviations, and Acronyms	19
Distribution List	20

List of Figures

Figure 1. FLEA utilized in SH-60 Seahawk crew seat (3).	3
Figure 2. Lumped-parameter human body model.....	4
Figure 3. Coupling between rotorcraft floor structure and seat-occupant model.	5
Figure 4. Comparison of the vertical seat-to-head vibration transmissibility characteristics computed from the proposed human body model with those upper and lower limits of experimental data from (4).....	6
Figure 5. Comparison of the vertical driving-point mechanical impedance characteristics computed from the proposed human body model with those upper and lower limits of experimental data from (4).....	7
Figure 6. Simulink control flow diagram for end-stop control.....	8
Figure 7. Typical rotorcraft pulse profile and deceleration limit for the seated occupant (3).	10
Figure 8. A lumped-parameter seat-occupant model.....	11
Figure 10. Baseline vs. MREA with Control for 50th percentile occupant.....	13
Figure 11. Baseline vs. MREA with Control for 95th percentile occupant.....	13
Figure 12. Finite element seat-occupant model.	15
Figure 13. Occupant kinematics and seat stroke from baseline simulation with passive seat damper.....	16

List of Tables

Table 1. Estimated body segment mass properties (5).	4
Table 2. Stiffness and damping coefficients of the human body segments.	5
Table 3. Control parameters.....	8
Table 4. Injury assessment criteria.....	11

Acknowledgments

This research work was performed under a research funding awarded by the Joint Aircraft Survivability Program Office (Project Number: JASP# V-13-02). The authors thank Dr. Norman Wereley, Professor of Aerospace Engineering and his research team at the University of Maryland, College park, MD for their help in the component research, development, analysis and testing of smart semi-active energy absorbers for rotorcraft crashworthiness enhancement.

1. Summary

Full spectrum crashworthiness for rotorcraft can be improved by adopting a holistic approach to crash survivability design. Full spectrum crashworthiness requirements can be met by system level design integration through a combination of crash kinetic energy attenuating seats, crashworthy sub-systems like crashworthy crew cabin structure, and other protection sub-systems for fire prevention and expedient egress. The focus of this research project is on crew-seat sub-system technologies that can mitigate injurious effects caused by crash loading. The crash energy management in crew seat is enabled by controlled seat-stroke that is typically accomplished by discrete energy absorbing devices. The objectives of this project are to conduct research and development, and demonstrate two novel seat energy absorber (EA) technologies using “smart” materials for enhanced rotorcraft crash safety: (1) Rotary Magneto-rheological EA (MREA) with magnetic bias, and (2) Magnetostrictive Friction Energy Absorber (MFEA). These EA devices will automatically adapt to stroking load based on occupant weight and crash severity and will have secondary benefit of vibration isolation. Both EAs will be evaluated to full-scale crash loads using an “iron-bird” (ruggedized) seat through sled testing in future in the final year of this project.

MREA uses magnetorheological fluid (typically hydraulic fluid with suspended micron-sized magnetizable particles) to adjust the fluid stiffness in a damper, and thereby absorbs and dissipates crash or impact energy. MFEA uses a magnetostrictive material such as Terfenol-D, which exhibits change in shape/length when subjected to changes in magnetization state. This technology has not been explored for crash energy absorption yet, and this project attempts to explore the viability of this technology for use in an adaptive crashworthy safety seat. This report presents a methodology to conduct analytical performance evaluations of these energy absorbers to determine the performance benefits of these devices as compared to passive energy absorbers. This analysis methodology is also used to help fine tune the design of these adaptive systems for different occupant sizes and crash severity levels. Typical rotorcraft vertical crash pulses, as recommended by rotorcraft crashworthiness requirements are used to assess crash injuries for a seated occupant. The injury criteria and tolerance levels for the biomechanical effects are discussed for each of the identified vulnerable body regions. This main focus of the analytical performance evaluations of these technologies is to keep the spinal injury loads within tolerable limits during vertical crash landings of a helicopter.

2. Introduction

Rotorcraft crew seats generally use passive energy absorbers to attenuate the vertical crash loads that are transmitted through the fuselage structure of the rotorcraft to the seated occupant (1) during a crash or hard impact landing event. These energy absorbers (EAs) include fixed-load energy absorbers (FLEAs), shown in figure 1 or variable load energy absorbers (VLEAs) (1–2). These passive energy absorbing devices are not capable of automatically adapting their load-stroke profile as a function of occupant weight or as a function of varying degree of impact severity during a crash or hard landing event. In the recent times, smart adaptive energy absorbing devices, such as magneto-rheological energy absorbers (MREAs), have emerged as an innovative solution for providing active crash protection by utilizing a continuously adjustable profile EA in a controlled manner during a crash event. MREAs can adapt their stroking load as a function of occupant weight and also can respond to various impact/shock excitation levels in combination with a semi-active feedback controller. By intelligently adjusting the load-stroke profile of the MREA as the seat strokes during a hard landing or crash event, MREAs have the capability of providing an optimal combination of a short stroking distance coupled with minimal lumbar loads with varying occupant weight and impact severity level. Furthermore, MREAs offer the unique ability to use the same seat suspension system for both shock isolation during hard landings or crash impacts and for vibration isolation during normal and extreme maneuvering flight conditions. This paper presents an analytical evaluation technique to determine the performance benefits of MREA devices as compared to passive energy absorbers. This analysis method can help to fine tune the design of these adaptive systems for different crash scenarios. This model will also help in evaluating control algorithms that can be used in rotorcraft crashworthy seat systems. In this study, a lumped-parameter human body model including lower leg in seated posture was developed for crash injury assessment simulation. Typical rotorcraft crash pulse, as recommended by rotorcraft crashworthiness requirements was used to assess crash injuries in different segments of the body of the seated occupant. The injury criteria and tolerance levels for the biomechanical effects are discussed for each of the identified vulnerable body regions such as the thoracic lumbar loads for different sized adults.

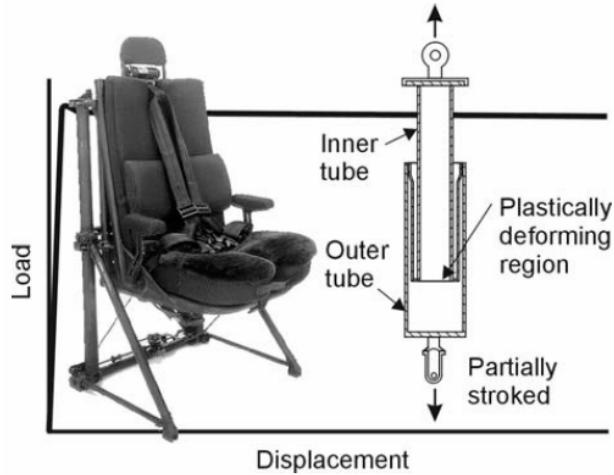


Figure 1. FLEA utilized in SH-60 Seahawk crew seat (3).

3. Model Development

Seated Human Model

Consider a human sitting upright in a rotorcraft crew seat. A variety of mathematical models have been proposed to describe the human body's response to vertical disturbances. In this study, Boileau's model (4) is used as a basic parameter model. However, Boileau's model was developed for "average" passenger comfort evaluation and it has no lower leg consideration which may be important for overall human body kinematics under extreme environment. To resolve this problem, the body segment mass was extracted from anthropometric specifications for dummy family (5) for the 5th percentile female (small female), 50th percentile male (average male), and 95th percentile male (large male). The proposed lumped parameter human body model, shown in figure 2, comprises six masses for the respective six body segments, coupled by linear/nonlinear elastic and damping elements. The six masses represent the following six body segments: the head and neck (m_1); the thorax (m_2); the abdomen (m_3); the pelvis (m_4); the thighs (m_5); and the calf and foot (m_6). The estimated segment mass properties (5) are summarized in table 1. The hand and arm masses (upper extremity) are not incorporated in the model assuming its negligible contributions to the whole-body biodynamic response. The stiffness and damping properties of the cervical spine are represented by k_1 and c_1 , those of the thoracic spine by k_2 and c_2 , those of the lumbar spine by k_3 and c_3 , while those of the buttocks and thighs on a seat by k_4 and c_4 as shown in figure 2. Also, there are two torsion stiffness and damping parameters for hip (k_5, c_5) and knee (k_6, c_6) joints (6). Manseau *et al.* (7) reported that the military boot has a significant effect on the complex lower leg injury severity. To take into account this boot effect, stiffness and damping parameters (k_b and c_b) were also implemented in the model as shown in

figure 2. These stiffness and damping parameters (8) are summarized in table 2 with the source of the data. Overall, this multi-body human model was developed at the U.S. Army Research Laboratory primarily for vertical impact injury assessment simulations in vehicular extreme environment scenarios such as crash or mine blast (9).

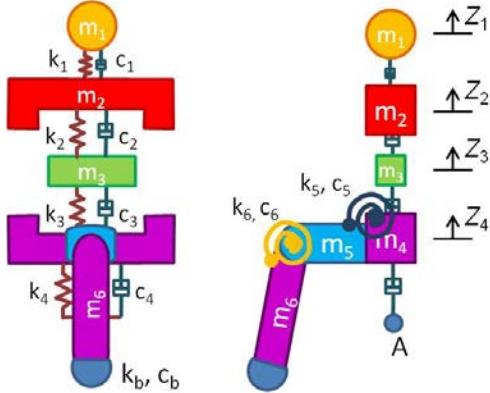


Figure 2. Lumped-parameter human body model.

Table 1. Estimated body segment mass properties (5).

Body Segment	Small (5th percentile) Female	Medium (50th percentile) Male	Large (95th percentile) Male
	Mass (kg)	Mass (kg)	Mass (kg)
Head (m_1)	4.30	5.10	5.68
Thorax (m_2)	17.50	28.79	37.90
Abdomen (m_3)	1.61	2.37	2.95
Pelvis (m_4)	6.98	11.41	16.04
Thigh (m_5)	11.83	17.23	21.65
Calf and foot (m_6)	6.00	11.66	18.24
Total	48.22	76.56	102.46

Table 2. Stiffness and damping coefficients of the human body segments.

	Stiffness	Damping	Source
Cervical spine (k_1, c_1)	310.0(kN/m)	400.0(N·s/m)	(4)
Thoracic spine (k_2, c_2)	183.0(kN/m)	4750.0(N·s/m)	
Lumbar spine (k_3, c_3)	162.8(kN/m)	4585.0(N·s/m)	
Buttocks (k_4, c_4)	90.0(kN/m)	2064.0(N·s/m)	
Hip joint (k_5, c_5)	Extension (N·m/rad): 68.8 Flexion (N·m/rad): 53.2·Exp(0.98×θ ₂)-53.2	100.0 (N·m·s/rad)	(6)
Knee joint (k_6, c_6)	Extension (N·m/rad): 90.5·Exp(2.0×θ ₃)-90.5 Flexion (N·m/rad): 95.0·Exp(4.32×θ ₃)-95.0	500.0 (N·m·s/rad)	
Boot (k_b, c_b)	300.47 (kN/m)	200.0 (N·s/m)	(8)

The conceptual model of the rotorcraft floor structure with a crew seat used in this study is shown in figure 3. The point ‘A’ in figure 3 shows the coupling between the seat-occupant model and the rotorcraft floor structure.

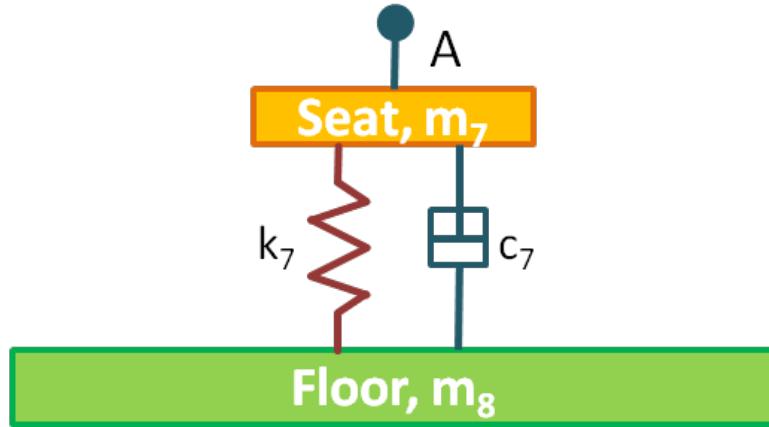


Figure 3. Coupling between rotorcraft floor structure and seat-occupant model.

4. Biodynamic Evaluation of Seated Human Model

The biodynamic responses of a seated human subjected to vertical vibration or shock exposure have widely been assessed in terms of seat-to-head (STH) transmissibility (TR), and driving-point mechanical (DPM) impedance (10). To evaluate these performance indices, the whole human body model, shown in figure 2, was implemented in the multi-body dynamic simulation software, (MSC/ADAMS) and each segment responses were simulated using the Vibration module in the software. The frequency step and frequency range of 0.5 Hz, and up to 100 Hz were selected, respectively.

4.1 STH Transmissibility (STH TR)

This function, STH TR is defined as the ratio of output head response to input seat excitation. It can be defined by the acceleration or displacement ratio. Therefore, TR can be expressed according to the above derivation as shown in the cited reference (10).

$$TR = \frac{Z_1(j\omega)}{Z_A(\omega)} \quad (1)$$

where ω is frequency, $Z_A(\omega)$ is input displacement amplitude from seat, and $Z_1(j\omega)$ is output displacement amplitude from head and neck m_1 . Figure 4 presents a comparison of the transmissibility magnitude characteristics calculated from the model with the mean and envelope of the experimental data from the cited reference (4).

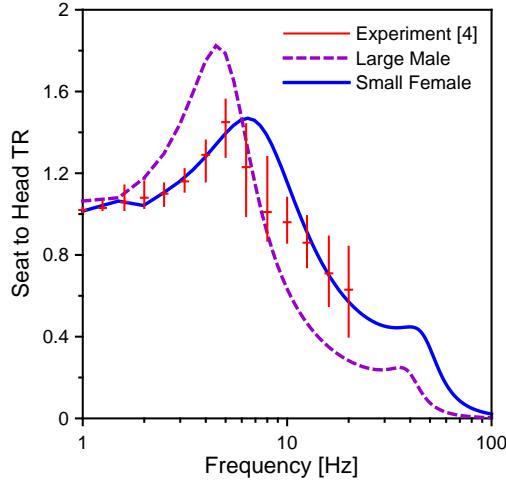


Figure 4. Comparison of the vertical seat-to-head vibration transmissibility characteristics computed from the proposed human body model with those upper and lower limits of experimental data from (4).

4.2 DPM Impedance (DPM IM)

This function, DPM impedance is defined as the ratio of driving force between pelvis and seat to the input velocity of the seat. Accordingly, IM can be represented as follows (10):

$$IM = \left| \frac{(k_4 + j\omega c_4)[Z_A(\omega) - Z_4(j\omega)]}{j\omega Z_A(\omega)} \right| \quad (2)$$

where ω is frequency, $Z_A(\omega)$ is input displacement amplitude from seat, and $Z_4(j\omega)$ is output displacement amplitude from pelvis m_4 . Figure 5 presents a comparison of the impedance magnitude characteristics calculated from the model with the mean and envelope of the experimental data from the reference (4).

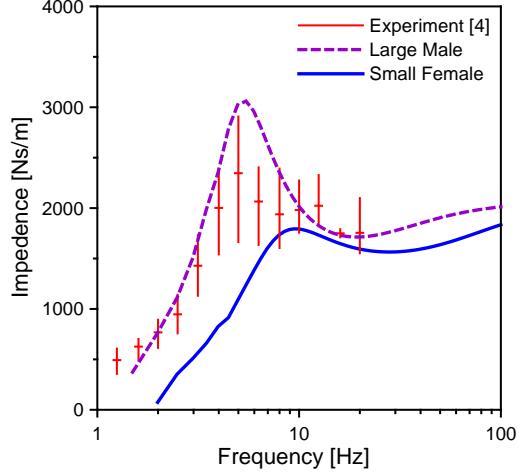


Figure 5. Comparison of the vertical driving-point mechanical impedance characteristics computed from the proposed human body model with those upper and lower limits of experimental data from (4).

5. Control Algorithm Development

For vibration isolation of seat damper, high damping will suppress the amplitude response, but worsen the vibration transmissibility. Low damping will improve the transmissibility, but the relative displacement between the seat and floor may be large enough to cause end-stop impacts especially for high shock input from crash event. If the shock input force does not cause the suspension mechanism to hit the end-stop buffers, a lower suspension damping may provide greater vibration isolation performance. However, for the input force from crash event, an adjustable damper, which can be switched manually or automatically between a high damping and low damping according to the passenger's weight or damper deflection, might be used. If the damper is generally set to soft mode so as to provide low transmissibility, and adjust to the hard mode only when end-stop impacts are likely to occur, the optimum performance might be achieved (11). End-stop impacts will occur whenever the relative displacement between the seat and floor exceeds certain value. If the damper is switched on whenever the relative displacement exceeds a pre-set displacement threshold, d_L , severe end-stop impacts might be prevented.

Figure 6 shows the semi-active control algorithm flow chart for Simulink/Matlab program. This control flow implements the multi-body dynamic model block (“adams_sub” block) of MSC/ADAMS for running co-simulation with the control scheme software plug-in. The input to the “adams_sub” block is damping force, and the three outputs from the block are the seat displacement, x , floor-pan absolute velocity, \dot{x}_0 , and the seat absolute velocity, \dot{x} . Considering the power limitation of Magnetorheological damper for semi-active skyhook control (figure 6), the maximum feedback force to the “adams_sub” block was set to 15kN using the “Saturation” block function.

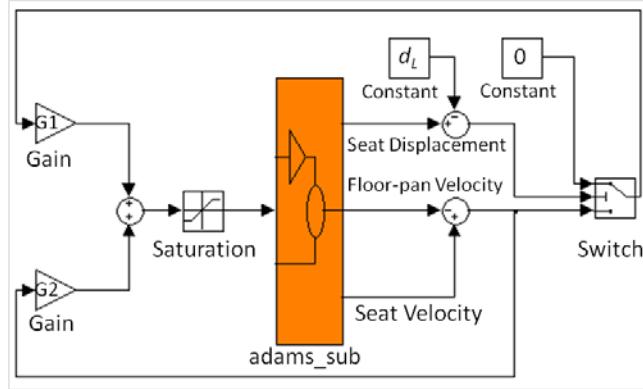


Figure 6. Simulink control flow diagram for end-stop control.

The control scheme can be expressed as:

$$Fd = \begin{cases} G2\dot{x}(\dot{x} - \dot{x}_0), & d_{seat} \geq d_L \\ (G1 + G2)\dot{x}(\dot{x} - \dot{x}_0), & d_{seat} < d_L \end{cases} \quad (3)$$

The control gains, G1 and G2 are functions of passenger weight, and the gains for this study are summarized in table 3 for the human body model.

Table 3. Control parameters.

Body Model	Small (5th percentile) Female	Medium (50th percentile) Male	Large (95th percentile) Male	Unit
G1	1	2	3	kN/(m/s)
G2	0.01	0.05	0.3	kN/(m/s)
d _L	335	335	335	mm

6. Rotorcraft Crash Pulse

Based on a study of survivable crash scenarios for U.S. Army helicopters during 1950's and 1960's, design guidelines and detailed requirements were developed for military crew seats as defined in MIL-S-85510(AS) (12) and for civil rotorcraft seats in Society of Automotive Engineers (SAE), AS8049 (13). Recently Full Spectrum Crashworthiness Criteria for rotorcraft have been published by the U.S. Army Research, Development and Engineering Command (RDECOM) (U.S. Army Aviation Applied Technology Directorate [AATD]) (14). Based on these published guidelines, crash pulse for vertical impacts of military helicopters with a $\Delta V_z = 42\text{ft/sec}$ (2, 14) was used for this research. A typical rotorcraft vertical impact crash pulse profile as shown schematically in figure 7 was utilized with seat-occupant model for the analytical evaluation of passive EA and semi-active MREA. The maximum deceleration, and the deceleration-time history relationship (pulse) developed for the design of a crashworthy seat system for a military helicopter are given below in figure 7. In figure 7, G_m refers to maximum deceleration; t_m is the time to reach maximum deceleration G_m ; and G_L is the limit-load deceleration. The deceleration of the occupant must be limited to a level, G_L such that the applied loads are of a humanly tolerable time-magnitude relationship. Once the seat-occupant system reaches this limit load deceleration (G_L), the seat strokes at constant load factor keeping the occupant's lumbar load within tolerable limits. After extensive analysis of crash injury data, it was determined that the limit-load deceleration level should be 14.5g (12). So, the crash energy absorbing systems (EAs) for military helicopter seats should be sized for a limit load that is 14.5 times the effective weight of the seat-occupant system including restraints and other body-worn items. This limit load factor was later verified by cadaveric testing and analysis as well (13). The limit load, L_L varies with the occupant-seat (O-S) system effective weight and it can be calculated as follows:

$$L_L = 14.5g \times W_{(O-S)eff} (\text{lb}) \quad (4)$$

Where $W_{(O-S)eff}$ (lb) is the effective occupant-seat system weight. For varying occupant sizes (5th percentile through 95th percentile occupants), this varying limit load can be calculated, and EA systems can be designed and controlled to the required stroking load keeping the stroke within allowable design limits.

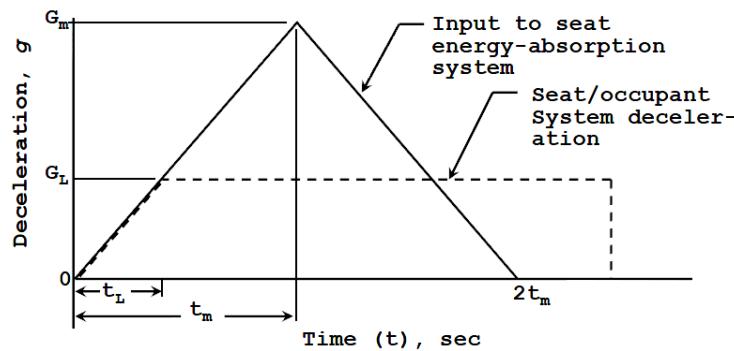


Figure 7. Typical rotorcraft pulse profile and deceleration limit for the seated occupant (3).

Note: $G_m = 48 \text{ g}$; $2t_m = 54 \text{ msec}$; $\Delta V_z = 42 \text{ ft/sec}$; and $G_L = 14.5 \text{ g}$

The complete model set-up for simulations are conceptually shown in figure 8 for the passive EA (Baseline — no control) and semi-active EA, MREA (with control). The control algorithm was implemented using co-simulation with seat-occupant dynamic model.

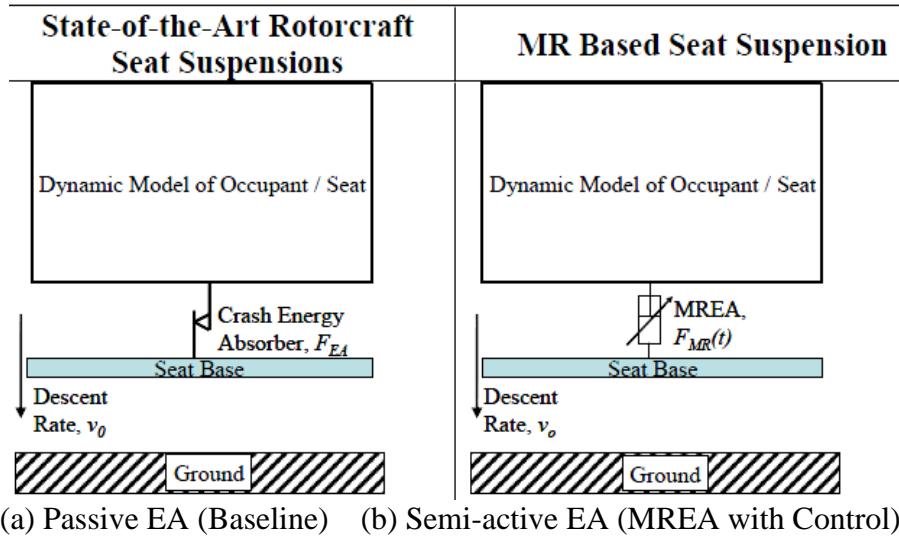


Figure 8. Schematic sketch of simulations for Passive EA and MREA (3).

7. Injury Assessment Criteria

The key injury assessment parameter such as the lumbar loads would be the primary focus in comparing the performance benefits of passive EA and MREA. The lumbar load injury assessment reference values (IARVs) as stipulated in the Full Spectrum Crashworthiness Criteria published by the AATD (14) were used

as reference (table 4) for evaluation of MREA through analysis. The IARVs for lumbar load injury criteria for tolerable limits were used for comparison of performance between the passive EA (Baseline) and MREA with Control cases.

Table 4. Injury assessment criteria.

Injury Assessment Parameter	IARV
Lumbar load	< 933 lb (4150 N) for 5th percentile < 1395 lb (6205 N) for 50th percentile < 1757 lb (7815 N) for 95th percentile (per Full Spectrum Crashworthiness Criteria guidelines [14])

8. Simulation Results and Discussion

The biodynamic model, shown in figure 2 and rotorcraft floor model, shown in figure 3 were combined and implemented in MSC/ADAMS as shown in figure 9. An active control element was implemented and designed to generate force in between floor-pan and seat. The non-linear human biodynamic model was co-simulated with Simulink control scheme plug-in, as shown in figure 6. “Co-Simulation” (co-operative simulation) is a simulation methodology that allows individual components to be simulated using different simulation tools running simultaneously and exchanging information in a collaborative manner. The nonlinear human body model in (MSC/ADAMS) was generated in Simulink accessible code (.m-file and .mdl-file, “adams_sub” block in figure 6) through ADAMS/Control module.

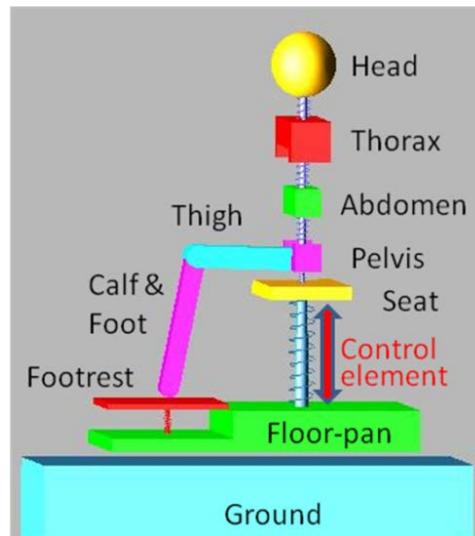


Figure 8. A lumped-parameter seat-occupant model.

Figures 10 through 12 show the simulation results for three cases, namely, 5th percentile, 50th percentile, and 95th percentile occupant models. Figure 10 shows the reduction of lumbar load for 5th percentile analysis case between the baseline (passive EA with no control) and MREA with control. In figure 10, the peak lumbar load for the Baseline case is 1477 lbf (exceeds the IARV limit), whereas the peak load for MREA with Control analysis case is 926 lbf (< 933 lbf [IARV]). Thus, it has been shown through analysis that by choosing an adaptive MREA with right type of control algorithm, it is possible to mitigate thoracic spinal injury (lumbar load is a measure of this injury) to a seated occupant in a rotorcraft vertical crash event. In figure 11 for the 50th percentile analysis case, the peak lumbar load is reduced from 2248 lbf (Baseline) to 1388 lbf (MREA with Control) keeping the lumbar load well within the IARV limit for this severe crash scenario. Also, in figure 12 for the 95th percentile occupant analysis case, it has been shown that the peak lumbar load can be reduced from 2342 lbf to 1748 lbf, which is well within the IARV limit. These analysis cases show that it is possible to optimize the adaptive MREA device with a proper control algorithm for the crash scenarios that are of interest to improve the safety and survivability in rotorcraft crashes.

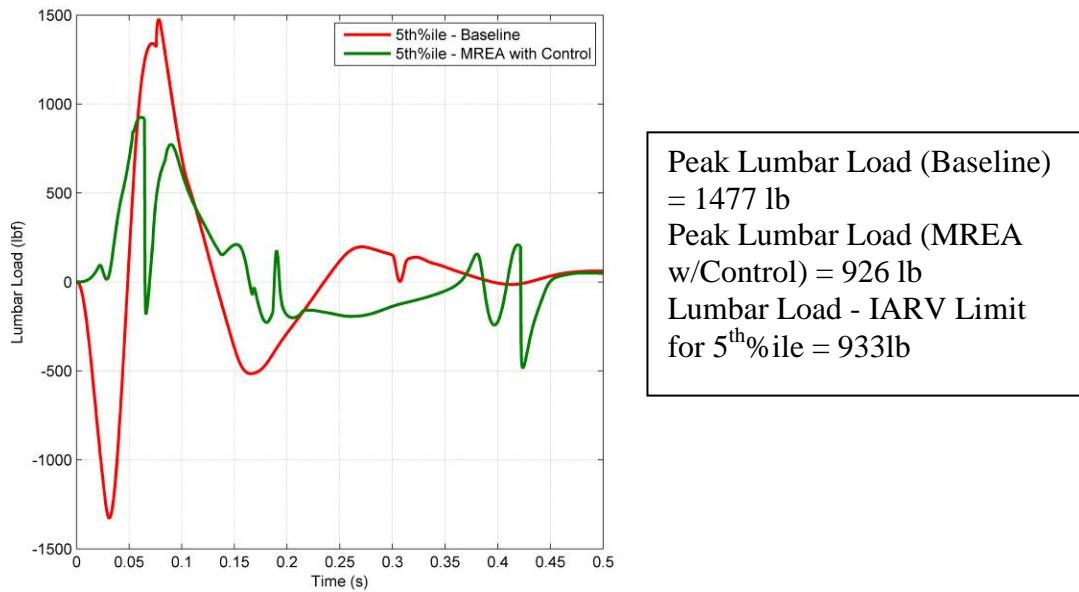
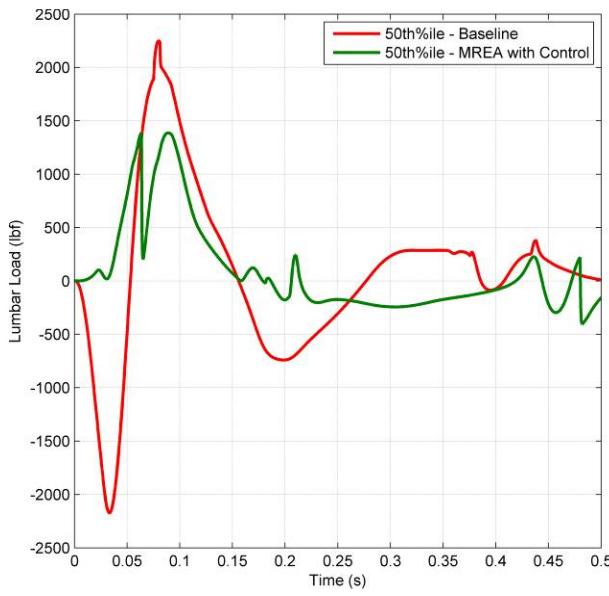
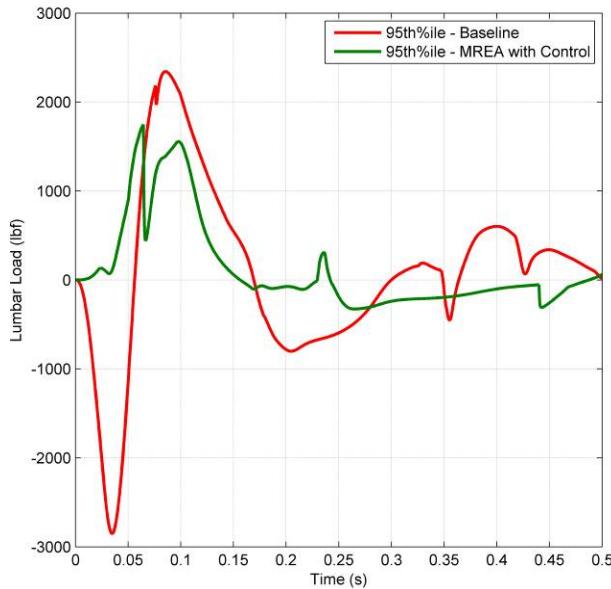


Figure 9. Baseline vs. MREA with Control for 5th percentile occupant.



Peak Lumbar Load (Baseline)
= 2248 lb
Peak Lumbar Load (MREA w/Control) = 1388 lb
Lumbar Load - IARV Limit for 50th%ile = 1395 lb)

Figure 10. Baseline vs. MREA with Control for 50th percentile occupant.



Peak Lumbar Load (Baseline)
= 2342 lb
Peak Lumbar Load (MREA w/Control) = 1748 lb
Lumbar Load - IARV Limit for 95th%ile = 1757 lb)

Figure 11. Baseline vs. MREA with Control for 95th percentile occupant.

9. Concluding Remarks from Multi-Body Simulations

This analytical research study proposes a lumped-parameter human body model including lower leg in seated posture for rotorcraft crashworthiness simulation and crash safety seat development with an adaptive semi-active seat energy absorber. The multi-body, lumped parameters were developed to represent a seated occupant in a rotorcraft interior environment. The upper extremity was neglected in the analysis model, since it is assumed that it has negligible effects on the overall bio-dynamics of the human body during a crash event. The developed models are applicable for an “average” human subject (close to a 50th percentile male), a small female 5th percentile human subject, and a large male 95th percentile human subject. The developed rotorcraft vehicle occupant model, with the chosen parameters, provides a reasonable estimate of the seat-to-head TR, and driving-point IM characteristics defined as applicable to target experimental values for ensuring bio-fidelity of the model. A generic rotorcraft vertical crash pulse as stipulated in military design standards was used to evaluate the performance of MREA seat energy absorber with a suitable control algorithm. The goal of this research was to establish a high fidelity lumped parameter seat-occupant model and a simulation methodology with a suitable control algorithm that can be used to evaluate and design adaptive magnetorheological energy absorbers for rotorcraft crashworthy safety seat application. The established model will also be helpful in the evaluation different types of control schemes for the efficient use of the adaptive MREAs to meet crew safety requirements with varying occupant sizes and vertical impact sink rates. An analysis methodology to co-simulate control algorithms together with lumped-parameter, multi-body seat-occupant system model with adaptive MREA device was demonstrated as well. It has been shown through this study that lumbar load reduction and consequent spinal injury mitigation can be achieved for all sizes of adults in a rotorcraft vertical crash event by using an adaptive semi-active seat energy absorber, such as a magnetorheological energy absorber with a suitable control algorithm to control the energy absorber actuation during the crash event.

10. Finite-Element Model Development

A seat-occupant system level test set-up with an “iron-bird” seat is being planned for energy absorber technology demonstration as part of this research project. Dynamic sled testing with full scale crash loads will be conducted for demonstration and verification of different types of seat damper technologies in future. In order to better understand occupant kinematics during vertical helicopter crashes and to conserve physical testing and cost, a more detailed finite-element model of the occupant-seat system has been developed. This finite element simulation model of a seated, belted (with five-point belt) occupant with a stroking seat, as shown in figure 13, will be

useful to study the occupant kinematics and the injury assessment values during crash sled simulations. The crash sled test results, when obtained, will be used for model analysis methodology correlation and tuning.

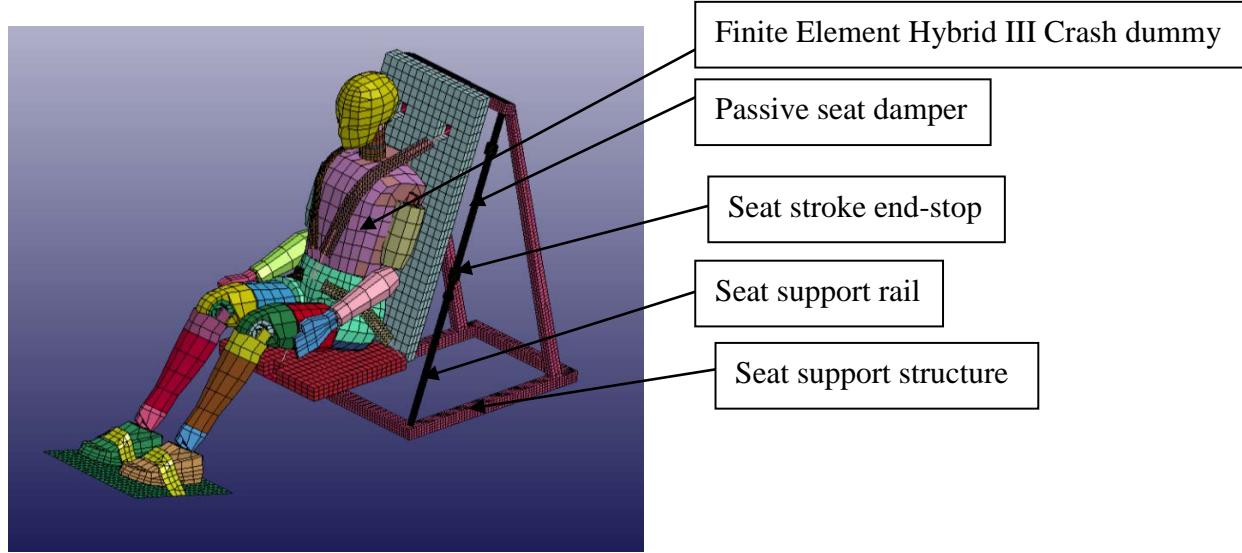


Figure 12. Finite element seat-occupant model.

The crash sled model, shown in figure 13 uses a Hybrid III 50th percentile crash dummy model that is available from Livermore Software Technology Corporation (LSTC) (15), and is compatible with LS-DYNA software, which is a nonlinear, large deformation dynamics analysis solver that was used to conduct simulations. The Hybrid III finite element crash dummy model closely represents the Hybrid III Anthropomorphic Test Device that is typically used in crash sled testing for injury assessment evaluations. The stroking seat model, shown in figure 14, can have a maximum stroke of 15 in before it hits the end-stop mechanism on the seat support rails. Figure 14 shows the end kinematic state of the seated occupant (50th percentile male) for a passive energy absorber (fixed load energy absorber) with a symmetrical triangular crash pulse of maximum 51 g and a time duration of 51 ms for maximum deceleration (51 g) (refer to figure 7). Also, in this model additional weight of 20 kg was added to the seat to represent typical Soldier borne equipment. As shown in figure 14, due to additional weight and crash severity, the passive energy absorber is not sufficient to absorb the crash energy within the available stroke of 15 in. An adaptive energy absorber such as the magnetorheological energy absorber would be able to dissipate the energy if the damper force can be varied to the rate of seat stroke during a crash event. Currently, the performance characterization of the adaptive EAs is being obtained through component testing. These load-deflection characteristics will be used in the developed model to study the injury assessment evaluations of different sizes of occupants for different crash severities in future.

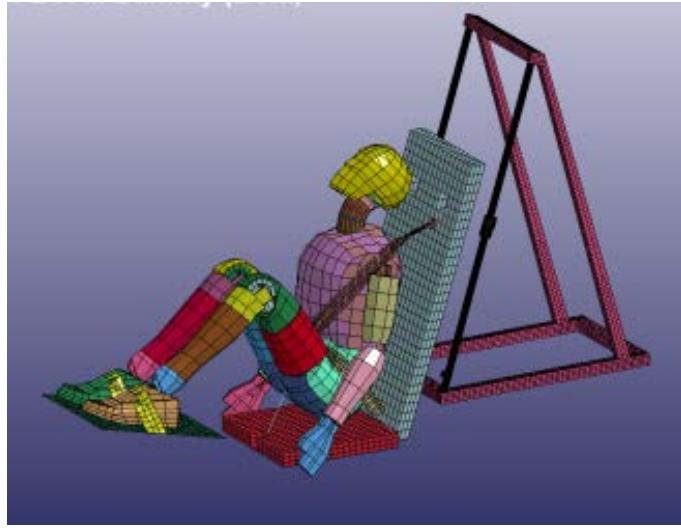


Figure 13. Occupant kinematics and seat stroke from baseline simulation with passive seat damper.

(Note: seat stroke mechanism hits end-stop).

11. Future Work

The project team intends to continue analytical injury assessment performance evaluations and integrate an adaptive control module for automatically adjusting MREA and MFEA devices. Additionally, the project team will conduct system level crash sled testing of the adaptive seat system to full-scale crash loads to demonstrate system performance. System level analyses and testing comparisons will be conducted with respect to baseline (fixed load energy absorber) technology. From this comparison, safety benefits estimation will be made using existing helicopter crash data with passive energy absorbers.

12. References

1. Richards, M.; Podob, R. Development of an Advanced Energy Absorber. *Proceedings of 35th Annual SAFE Symposium*, 1997.
2. Desjardins, S. P.; Zimmerman, R. E.; Bolukbasi, A. O.; Merritt, N. A. *Aircraft Crash Survival Design Guide Vol. IV – Aircraft Seats, Restraints, Litters, and Cockpit/Cabin Delethalization*; USAAVSCOM Technical Report 89-D-22D; Aviation Applied Technology Directorate, 1989, pp 45–58, 83–109, 165.
3. Hiemenz, G. J. Semi-Active Magnetorheological Seat Suspensions for Enhanced Crashworthiness and Vibration Isolation of Rotorcraft Seats. Ph.D. dissertation, University of Maryland (College Park, MD), 2007.
4. Boileau, P.-É., Rakheja, S. Whole-Body Vertical Biodynamic Response Characteristics of the Seated Vehicle Driver, Measurement and Model Development. *International Journal of Industrial Ergonomics* **1998**, 22, 449–472.
5. Herman, I. P. *Physics of the Human Body*; Springer-Verlag Berlin: Heidelberg, NY, 2007, pp 16–17.
6. Ciarlet, P. G. *Handbook of Numerical Analysis, Volume XII Special Volume: Computational Models for the Human Body*, Ayache, N., Ed.; Elsevier: North Holland, 2004, p. 392.
7. Manseau, J.; Keown, M. Development of an Assessment Methodology for lower leg Injuries Resulting from Antivehicular Blast Landmines. *IUTAM Proceedings on Impact Biomechanics: From Fundamental Insights to Applications*, Springer, the Netherlands, pp. 33–40, 2005.
8. Cikajlo, I.; Matjačić, Z. The Influence of Boot Stiffness on Gait Kinematics and Kinetics During Stance Phase. *Ergonomics* **2007**, 50 (12), 2171–2182.
9. Yoo, J. H.; Murugan, M.; Le, D., Development of a Lumped-Parameter Occupant Injury Assessment Model for Vehicular Blast Effects Simulation. *Proceedings of the ASME 2012 Conference on Smart Materials, Adaptive Structures and Intelligent Systems*, Stone Mountain, GA, 19–21 September, 2012.
10. Cho-Chung, L.; Chi-Feng, C. A Study on Biodynamic Models of Seated Human Subjects Exposed to Vertical Vibration. *International Journal of Industrial Ergonomics* **2006**, 36, 869–890.

11. Wu, X.; Griffin, M. J. A Semi-Active Control Policy to Reduce the Occurrence and Severity of End-Stop Impacts in a Suspension Seat with an Electrorheological Fluid Damper. *Journal of Sound and Vibration* 1997, 203 (5), 781–793.
12. MIL-S-85510(As). *Military Specification, Seats, Helicopter Cabin, Crashworthy, General Specification For.* **1981**.
13. SAE, AS8049A. *Performance Standard For Seats in Civil Rotorcraft, Transport Aircraft, and General Aviation.* **1990, 1997**.
14. U.S. Army RDECOM. *Full Spectrum Crashworthiness Criteria for Rotorcraft*; RDECOM TR 12-D-12; Aviation Applied Technology Directorate: Fort Eustis, Virginia, December 2011.
15. LS-DYNA Keyword User's Manual, Version 971, Volume I, May 2007, Livermore Software Technology Corporation (LSTC).

List of Symbols, Abbreviations, and Acronyms

AATD	Army Aviation Applied Technology Directorate
DPM	Driving-Point-Mechanical
DPM IM	Driving-Point-Mechanical Impedance
EA	energy absorber
FLEA	fixed-load energy absorber
IARV	injury assessment reference value
LSTC	Livermore Software Technology Corporation
MFEA	Magnetostrictive Friction EA
MR	magneto-rheological
MREA	magneto-rheological energy absorber
O-S	occupant-seat
RDECOM	Research, Development and Engineering Command.
SAE	Society of Automotive Engineers
STH	seat-to-head
STH TR	seat-to-head transmissibility
VLEA	variable load energy absorber
<i>c</i>	damping
<i>g, G</i>	gravitational acceleration
<i>k</i>	stiffness
<i>m</i>	mass
<i>ms</i>	milliseconds
<i>t</i>	time

NO. OF
COPIES ORGANIZATION

1 DEFENSE TECHNICAL
(PDF) INFORMATION CTR
DTIC OCA

2 DIRECTOR
(PDF) US ARMY RSRCH LAB
RDRL CIO LL
IMAL HRA MAIL & RECORDS MGMT

1 GOVT PRINTG OFC
(PDF) A MALHOTRA

2 DIR USARL
(PDF) RDRL VTM
D LE
M MURUGAN